hep-ph/9710500 28 Oct 1997

The $\gamma^*\gamma^*$ Total Cross Section and the BFKL Pomeron at the 500 GeV e^+e^- Linear Collider

Jochen Bartels[a], Albert De Roeck[b], Carlo Ewerz[a], Hans Lotter[a,1]

[a] II. Institut für Theoretische Physik, Universität Hamburg,
Luruper Chaussee 149, D-22761 Hamburg[2]
[b] Deutsches Elektronen-Synchrotron DESY, Notkestr. 85, D-22603 Hamburg

Abstract: We present a numerical estimate of the $\gamma^*\gamma^*$ total cross section at the designed 500 GeV e^+e^- Linear Collider, based upon the BFKL Pomeron. We find that the event rate is substantial provided electrons scattered under small angles can be detected, and a measurement of this cross section provides an excellent test of the BFKL Pomeron.

1 Introduction

In the past years, the BFKL Pomeron [1] has been intensively investigated, in particular in the context of small–x deep inelastic electron-proton scattering at HERA. Whereas the use of this QCD leading logarithmic approximation for the proton structure function is affected by serious theoretical difficulties, it has been argued [2] that the observation of forward jets near the proton beam provides a much more reliable test of the BFKL Pomeron. The main reason for this lies in the fact that the forward jet cross section involves only a single large momentum scale, namely the transverse momentum of the forward jet which is chosen to be equal or close to the virtuality of the photon. In the structure function F_2, on the other hand, the BFKL Pomeron feels both the large momentum scale of the photon mass and the lower factorization scale. In addition, the diffusion in $\log k_T^2$ always leads to a nonzero contribution of small transverse momenta where the use of the leading logarithmic approximation becomes doubtful. A numerical estimate shows that for the forward jets at HERA [3] the contribution from this dangerous infrared region is reasonably small, whereas in the case of F_2 [4] the situation is much less favorable. As to the experimental situation, recent analyses of HERA data [5, 6, 7] on the production of forward jets shows a very encouraging agreement between data and the theoretical prediction.

In this contribution we would like to point out that also e^+e^- linear colliders, in particular the linear colliders with a rather high luminosity, offer an excellent opportunity to test the BFKL prediction. The process to be looked at is the total cross section of

[1] Now at Trinkaus & Burkhardt KGaA, Königsallee 22, D-40212 Düsseldorf

[2] Supported by Bundesministerium für Forschung und Technologie, Bonn, Germany under Contract 056HH93P(5).

$\gamma^*\gamma^*$ scattering. The measurement of this cross section requires the double tagging of both outgoing leptons close to the forward direction. By varying the energy of the tagged leptons it is possible to probe the total cross section of the subprocess $\gamma^*\gamma^*$ from low energies up to almost the full energy of the e^+e^- collider. For sufficiently large photon virtualities we again have a situation with only large momentum scales. In other words, photons with large virtualities are objects with small transverse size, and it is exactly this situation for which the BFKL approximation should be considered most reliable. The energy dependence of this cross section, therefore, should be described by the power law of the BFKL Pomeron.

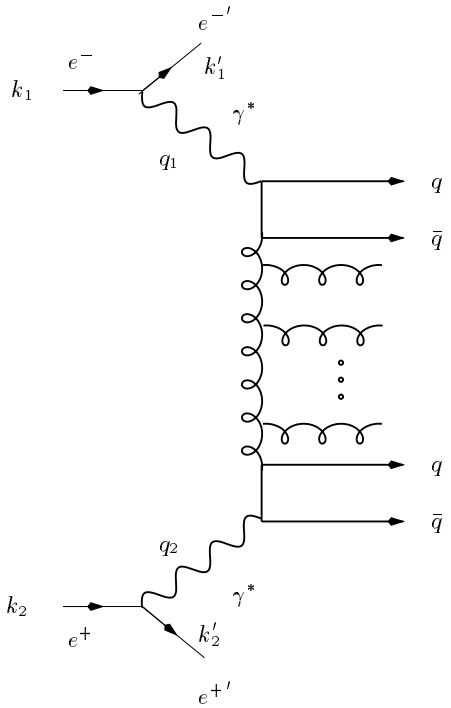

Figure 1: Feynman diagram for the process $e^+e^- \to e^+e^-$ + anything.

From the theoretical point of view it is clear that we want the photon masses to be large. On the other hand, because of the photon propagators, the e^+e^- cross section for this final state (i. e. the event rate for the process under discussion) falls off very rapidly with increasing photon masses. Therefore, one cannot afford to have too large photon virtualities. As a compromise, we chose the range of 5 to 200 GeV^2 (for experimental considerations see further below). As to the energies of the $\gamma^*\gamma^*$ subprocess, we can in principle go up to almost the full collider energies. From the theoretical side, however, it is important to estimate the diffusion in the internal transverse momenta k_T. In the center of the BFKL ladders (Fig.1), the distribution in $\log k_T^2$ is given by a Gaussian, with center at $\log Q^2$ (if we chose, for simplicity, both photon virtualities to be equal), and with the width growing linearly with the square root of rapidity. As soon as the small-k_T part of

the Gaussian reaches the confinement region the BFKL prediction (which is based upon a leading–log calculation) becomes unreliable. Corrections to the BFKL Pomeron, in particular those which are expected to restore unitarity are no longer small. Qualitatively they are expected to reduce the growth of the cross section with increasing energy. Below we will argue that this energy region can be reached at the linear collider. In other words, at highest energies for the $\gamma^*\gamma^*$ subprocess, a deviation from the power–rise of the BFKL Pomeron might become visible.

This note is based mainly on [8]. Here we give a more detailed analysis of event rates and their dependence on experimental resolution. Moreover, we propose a more refined way to extract a clean BFKL signal from the data. This is done by considering event samples in which the virtualities of the two photons are of the same order. We introduce a parameter that measures how much the virtualities differ. This parameter is easily accessible experimentally, and we give expected event rates for different parameter values.

The investigation of the $\gamma^*\gamma^*$ total cross section as a probe of BFKL dynamics has independently been advocated by Brodsky et al. [9]. The cross section formulae obtained there are in perfect agreement with our results presented here in section 2. The cross section has also been discussed by Bialas et al. within the framework of the colour dipole picture of the BFKL Pomeron [10].

2 Cross Section Formulae

The theoretical prediction of the cross section is based on the high energy behaviour of the diagrams shown in Fig. 1. Let us first define suitable variables. In analogy to DIS kinematics we chose the scaling variables

$$y_1 = \frac{q_1 k_2}{k_1 k_2}, \quad y_2 = \frac{q_2 k_1}{k_1 k_2} \tag{1}$$

and

$$x_1 = \frac{Q_1^2}{2 q_1 k_2}, \quad x_2 = \frac{Q_2^2}{2 q_2 k_1} \tag{2}$$

where the photon virtualities are, as usual, $Q_i^2 = -q_i^2$ $(i = 1, 2)$. Energies are denoted by $s = (k_1 + k_2)^2$ and $\hat{s} = (q_1 + q_2)^2 \approx s y_1 y_2$. With our definitions of the scaling variables we have $Q_i^2 = s x_i y_i$ $(i = 1, 2)$. We consider the limit of large Q_1^2, Q_2^2, and $\hat{s}$ with

$$Q_1^2,\, Q_2^2 \ll \hat{s}. \tag{3}$$

The calculation is straightforward and, neglecting terms of the order of $Q_i^2/\hat{s}$, leads to the following result:

$$\frac{d\sigma^{e^+e^-}}{dQ_1^2 dQ_2^2 dy_1 dy_2} = \frac{\alpha_{em}^2}{16\pi y_1 Q_1^4} \frac{\alpha_{em}^2}{16\pi y_2 Q_2^4} \int \frac{d\nu}{2\pi^2} \exp\left[\log s \frac{y_1 y_2}{\sqrt{Q_1^2 Q_2^2}} \cdot \chi(\nu)\right] \times$$

$$\times \left[(1-y_1) W_L^{(1)}(\nu) + \frac{1+(1-y_1)^2}{2} W_T^{(1)}(\nu) \right]$$
$$\times \left[(1-y_2) W_L^{(2)}(-\nu) + \frac{1+(1-y_2)^2}{2} W_T^{(2)}(-\nu) \right] \qquad (4)$$

with $\chi(\nu) = (N_c \alpha_s/\pi)[2\psi(1) - \psi(1/2+i\nu) - \psi(1/2-i\nu)]$ and we have introduced the invariant functions:

$$W_L^{(i)}(\nu) = \sum_f q_f^2 \alpha_s \, \pi^2 \sqrt{2} \, 8 \frac{\nu^2 + \frac{1}{4}}{\nu^2+1} \frac{\sinh \pi\nu}{\nu \cosh^2 \pi\nu} (Q_i^2)^{\frac{1}{2}+i\nu} \qquad (5)$$

$$W_T^{(i)}(\nu) = \sum_f q_f^2 \alpha_s \, \pi^2 \sqrt{2} \, 4 \frac{\nu^2 + \frac{9}{4}}{\nu^2+1} \frac{\sinh \pi\nu}{\nu \cosh^2 \pi\nu} (Q_i^2)^{\frac{1}{2}+i\nu} \qquad (6)$$

Here q_f is the quark charge, and in our calculations the sum over (massless) flavours goes up to four. For the scale of the strong coupling constant we use $\sqrt{Q_1^2 Q_2^2}$ ($\alpha_s(M_Z^2) = 0.12$).

Before we turn to the discussion of numerical results, let us estimate the diffusion of internal transverse momenta into the infrared region. In the center of the BFKL ladders (Fig. 1), the width of the Gaussian distribution of $\log k_T^2$ is given by [3]

$$\Delta = \sqrt{< (\log k_T^2 - < \log k_T^2 >)^2 >} = \sqrt{7 \frac{N_c \alpha_s}{\pi} \zeta(3) \log s/s_0} \qquad (7)$$

with

$$s_0 = \frac{\sqrt{Q_1^2 Q_2^2}}{y_1 y_2} \, . \qquad (8)$$

For a typical value $Q_1^2 = Q_2^2 = 10\,\mathrm{GeV}^2$, and $\alpha_s = 0.22$ one finds, for the maximal value $Y = \log s/s_0 = 10$ at the 500 GeV e^+e^- Linear Collider, $\Delta = 4.2$ which means that the diffusion reaches down to $k_T^2 \approx 0.15$ GeV^2. Compared to the forward jets at HERA [3] where the corresponding value lies above $1\,\mathrm{GeV}^2$, we now have to expect a substantially larger contribution from the small-k_T region: this should lead to a lowering of the BFKL power behaviour of the cross section. In other words, one might be able to see the onset of unitarity corrections to the BFKL Pomeron.

3 Cross Section at the 500 GeV e^+e^- Linear Collider

Starting from eqs. (4)–(6) we have calculated the differential cross section for different values of the logarithm of the subenergy $Y = \log s/s_0$. In order to illustrate the BFKL power law, we have multiplied the cross section by $y_1 y_2$. In Fig. 2 we show the results for the 500 GeV Next Linear Collider. On the left hand side we display the e^+e^- cross section for $Q_1^2 = Q_2^2 = 10\,\mathrm{GeV}^2$. The right hand side shows the cross section for $Q_1^2 = Q_2^2 = 25\,\mathrm{GeV}^2$. For comparison, we have plotted on the left in each figure the corresponding

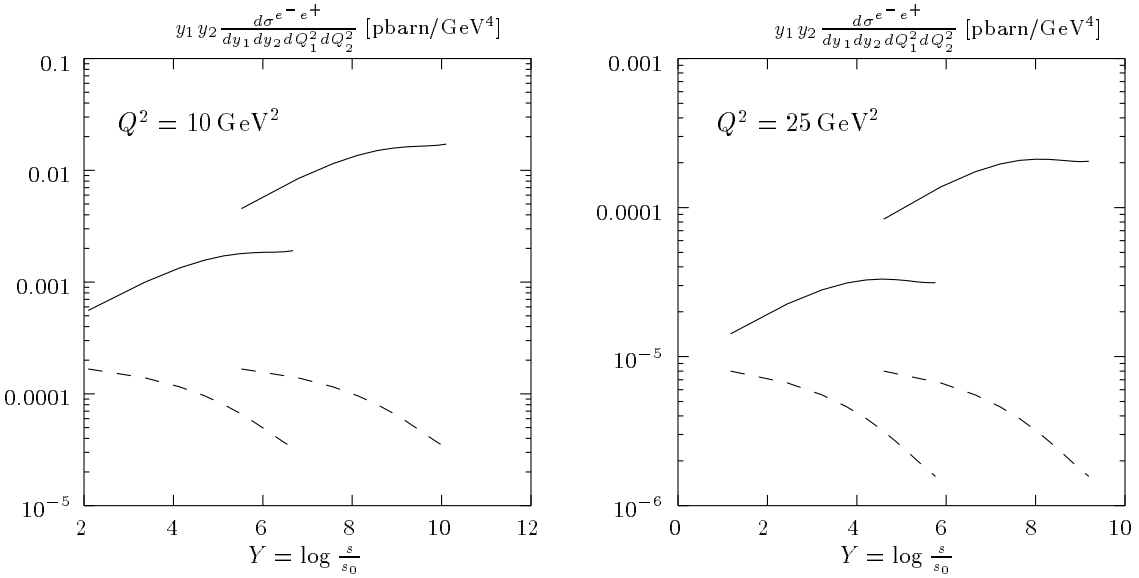

Figure 2: The differential e^+e^- total cross section, multiplied by y_1y_2, as a function of the rapidity $Y = \log s/s_0$. The full curves denote the numerical calculation based upon eq. (4) and the dashed lines represent the 2–gluon approximation (no gluon production between the two quark pairs). The two curves on the left in each figure are for LEP I, the ones on the right for the 500 GeV e^+e^- Linear Collider. We have chosen $y_1 = y_2$ and $Q_1^2 = Q_2^2 = 10\,\mathrm{GeV}^2$ (left hand figure) resp. $Q_1^2 = Q_2^2 = 25\,\mathrm{GeV}^2$ (right hand figure).

cross sections at LEP I (91 GeV e^+e^-). Due to the larger energy, the cross sections at the 500 GeV e^+e^- Linear Collider are considerably larger. The much higher design luminosity of the Linear Collider will lead to an even larger difference in event rates. The full curves represent the results based upon (4)–(6). The dashed lines denote the process in which there is no gluon production between the two fermion pairs (2–gluon approximation). This process is the one of lowest order in α_s that gives a sizable contribution to the cross section, since the quark–box diagram is strongly suppressed at high energy and can be neglected. Therefore, we compare our BFKL resummed prediction with this fixed order cross section.

From the curves in Fig. 2 one recognizes the typical BFKL power-like energy behaviour, but there is some damping at large rapidity (large y_i) due to the photon flux factors in (4). In the 2–gluon cross section this effect even leads to a decrease at large rapidity Y. The BFKL predictions are well above the 2–gluon curves, up to more than an order of magnitude. Comparing the right hand side of Fig. 2 with the left hand side we find that by increasing Q^2 from 10 to 25 GeV^2 the cross section decreases by two orders of magnitude. As seen from (4), the cross section scales with $1/Q^6$, and there is an additional decrease at larger Q^2 due to the Q^2-dependence of $\alpha_s(Q^2)$. Event rates for the 500 GeV e^+e^- Linear Collider are shown in Fig. 3, taking $3 \cdot 10^7$ s/year and assuming a luminosity of $\mathcal{L} = 10^{33}\,\mathrm{cm}^{-2}\mathrm{s}^{-1}$. Due to the limit in time of data taking periods, experiment and accelerator

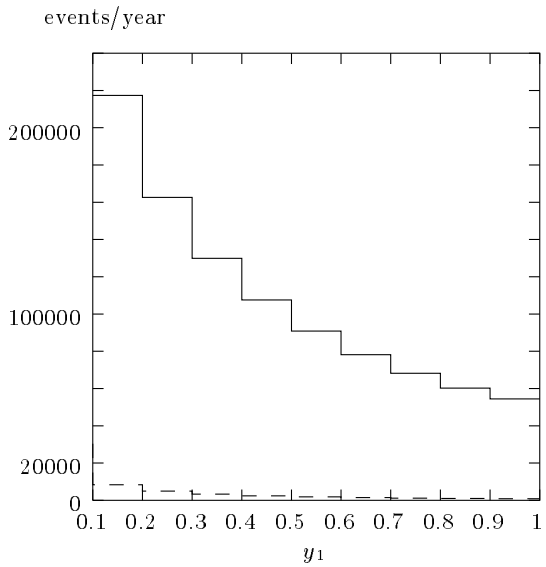

Figure 3: The total number of events per year ($3 \cdot 10^7$s), as a function of y_1. The variables Q_i^2 ($5 < Q_i^2 < 200$ GeV^2) and y_2 ($0.1 < y_2 < 0.9$) are integrated. The solid curve shows the results of the BFKL calculation and the dashed curve represents the 2–gluon result.

efficiency, this corresponds effectively to several years of operation of the accelerator. In Q_1^2 and Q_2^2 we integrate from 5 to 200 GeV^2, and for the y_1-variable we have chosen 9 bins, as indicated in the figure. The other y-variable is integrated from 0.1 to 1.0. The rapidity of the subprocess $\gamma^*\gamma^*$ is restricted by $\log s/s_0 > 2$. The event rate calculations are based upon Monte Carlo integration of the phase space, and the accuracy is of the order of 5%.

4 Experimental Restrictions and Event Rates

Due to experimental restrictions, however, these event rates can only give a first impression and not more. The measurement of the total cross section of $\gamma^*\gamma^*$ scattering can be made at existing and future e^+e^- colliders using so called "double tag" events. These are events where both outgoing leptons are detected and some hadronic activity is observed in the central detector. The Q^2 value of the virtual photon emitted from the lepton is $Q^2 = 2E_bE_{tag}(1-\cos\theta_{tag}) = 4E_bE_{tag}\sin^2\frac{\theta_{tag}}{2}$, with E_{tag} and θ_{tag} the energy and angle of the tagged lepton, and E_b the energy of the incident lepton. The variable y is given by $y = 1-(E_{tag}/E_b)\cos^2\frac{\theta_{tag}}{2}$. Combination of the two relations leads to the convenient equation

$$Q^2 = 4E_b^2(1-y)\tan^2\frac{\theta_{tag}}{2} \tag{9}$$

which holds for any of the two incoming leptons. Experiments at LEP tag electrons down to about 25 mrad [11] leading to Q^2 values as low as to $1\,\mathrm{GeV}^2$. For Q^2 values of 5 GeV^2 the electrons are scattered under an angle of 60 mrad, well within the forward detector acceptance of the LEP experiments. In order to reach such Q^2 values at a 500 GeV e^+e^- Linear Collider, the scattered leptons need to be detected down to 10 mrad. For photons of virtuality $20\,\mathrm{GeV}^2$ angles down to about 15–20 mrad need to be covered. According to the conceptual design report [12], the acceptance of the forward endcap electromagnetic calorimeters is foreseen to go down to angles of 80 mrad, leading to minimum reachable Q^2 values in the range of $60 - 80\,\mathrm{GeV}^2$.

One of the main problems in going down to smaller angles at the 500 GeV e^+e^- Linear Collider will be e^+e^- pair production. At the interaction point beam-beam effects cause production of beamstrahlung, which is very intense and collimated in a small cone around the beam axis. It will increase the background of e^+e^- pairs produced by two colliding real photons, which has been studied in [13]. The studies indicate that tagging of scattered electrons down to angles of 30 mrad is within reach. These electrons could be detected with the proposed small angle calorimeters, designed to measure the luminosity, with acceptance in the region $30 - 55$ mrad.

The y values reached in present single tagged analysis at LEP are in the range $y < 0.25$. However using double tagged events the background should be kept well under control also for larger y values, and therefore values of $y = 0.5$ or more, which lead to a large mass system for the hadronic final state and, correspondingly, to an extended ladder, are a realistic goal. Note that for all calculations presented here no requirement on the detection of the hadronic final state was made. Experimentally it is likely that some (very weak) cuts will have to be applied to discriminate the signal from background, which will reduce the rates somewhat.

In order to incorporate these conditions into our calculation of event rates for the 500 GeV e^+e^- Linear Collider, we have repeated the previous calculations with more realistic kinematical cuts. We impose the constraints $\theta_{tag} > 30$ mrad (Fig. 4, left) and $\theta_{tag} > 80$ mrad (Fig. 4, right), and we require $E_{tag} > 20$ GeV (i. e. approximately $y_i < 0.9$). Further restrictions are $2.5 < Q_i^2 < 200\,\mathrm{GeV}^2$ and $\log s/s_0 > 2$. In particular for smaller y_1 the event rate is substantially lower than the corresponding one in Fig. 3. (Fig. 3 shows event rates corresponding to 30000 pb^{-1}. To compare with numbers there, we thus have to multiply numbers in Fig. 4 by 30.) This shows the importance of the angle cut. Clearly, $\theta_{tag} = 30\,\mathrm{mrad}$ looks highly desirable. For $\theta_{tag} = 80$ mrad, the Q^2 values at the 500 GeV e^+e^- Linear Collider are rather large, reducing very strongly the event rate. The suppression of the small-y region in the right hand diagram of Fig. 4 results from the upper limit of the Q^2 range taken.

Further, we have computed a few integrated event rates. The results are shown in Table 1. We have integrated $2.5 < Q_i^2 < 200\,\mathrm{GeV}^2$, $0.1 < y_i < 1.0$, with the constraints $E_{tag} > 20$ GeV, $\log s/s_0 > 2$, and for the detector angles we have chosen $\theta_{tag} > 20 - 100$ mrad. For the smallest angles the ratio of BFKL to 2–gluon cross section is around 60. Note that according to the present design, the detector will not measure electrons with angles between 55 and 80 mrad, due to the mask to shield against background. For angles

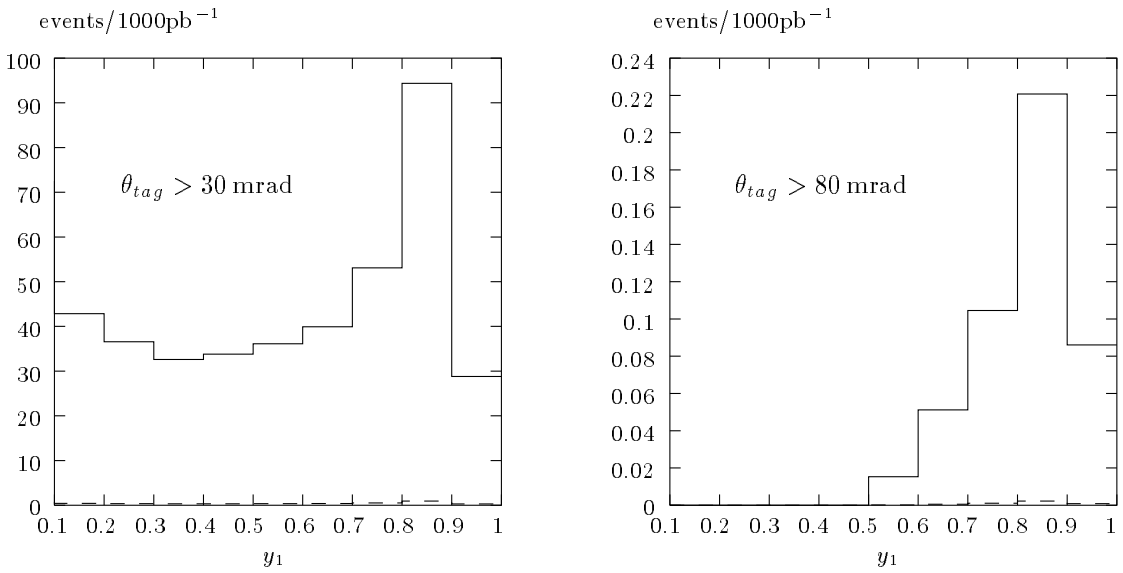

Figure 4: The total number of events per 1000 pb^{-1} with detector cuts in angle taken into account. This would typically correspond to one month of data taking at the design luminosity. We have chosen $E_{tag} > 20$ GeV, $\log s/s_0 > 2$, $2.5 < Q_i^2 < 200$ GeV^2. The acceptance cuts are $\theta_{tag} > 30\,$mrad (left) and $\theta_{tag} > 80\,$mrad (right). The y–binning is the same as in fig. 3. Solid lines are again the prediction based on BFKL, dashed lines represent the 2–gluon exchange.

$\theta_{tag,min}$	BFKL	2–gluon
20 mrad	2724	46
30 mrad	324	12
40 mrad	67	3.6
50 mrad	19	1.1
60 mrad	4.8	0.24
70 mrad	1.3	0.059
80 mrad	0.46	0.020
90 mrad	0.17	0.0074
100 mrad	0.063	0.0029

Table 1: Total event rates per 1000 pb^{-1} for different values of $\theta_{tag,min}$. We have chosen $E_{tag} > 20$ GeV, $\log s/s_0 > 2$, $2.5 < Q_i^2 < 200$ GeV^2.

above 80 mrad the BFKL cross section is by a factor of 23 larger than the 2–gluon cross section, but the limitation in Q^2 strongly affects the rate as discussed above. From this we conclude that, mainly because of the high luminosity of the 500 GeV e^+e^- Linear Collider, such a machine offers an excellent possibility to observe the BFKL Pomeron, provided the detectors can reach small angles down to about $20 - 30$ mrad.

So far, we have calculated event rates applying only the cuts $2.5 < Q_i^2 < 200$ GeV^2 for each of the photons. Strictly speaking, the BFKL calculation is applicable only for $Q_1^2/Q_2^2 = \mathcal{O}(1)$. For this kinematic region there is no DGLAP evolution between the two quark loops, and the BFKL results have to be compared to the 2–gluon exchange. For the full region $2.5 < Q_i^2 < 200$ GeV^2 this may be a rather crude approximation, and in a future step our analysis will have to be refined by using a background calculation based upon DGLAP evolution. For the moment, we propose to circumvent this difficulty by introducing an additional cut parameter ρ limiting the ratio of the two virtualities,

$$\frac{1}{\rho} < \frac{Q_1^2}{Q_2^2} < \rho\,. \tag{10}$$

This cut can easily be applied experimentally because we consider double tagged events. The closer to 1 the value chosen for ρ is the cleaner will be the BFKL sample obtained. Lowering ρ of course restricts phase space and thus lowers the number of events expected. The high luminosity of the 500 GeV e^+e^- Linear Collider will nevertheless make a value for ρ reasonably close to 1 affordable.

In Table 2 we present event rates for an acceptence angle of $\theta_{tag} > 30$ mrad, an integrated luminosity of $1000\,\mathrm{pb}^{-1}$, and different values of ρ. We have also varied the tagging energy of the electron E_{tag} to larger, i. e. less optimistic, values. The value $\rho = \infty$ corresponds to removing the additional cut and leads to the event rates discussed above. Having in mind the high luminosity of the 500 GeV e^+e^- Linear Collider, the

	$E_{tag} > 20\,\mathrm{GeV}$	$E_{tag} > 50\,\mathrm{GeV}$	$E_{tag} > 100\,\mathrm{GeV}$
$\rho = \infty$	324 (12)	159 (9)	72 (6)
$\rho = 3$	188 (9)	122 (7)	63 (5)
$\rho = 2$	122 (6)	87 (5)	47 (4)
$\rho = 1.5$	65 (4)	51 (3)	31 (3)

Table 2: Total event rates for $1000\,\mathrm{pb}^{-1}$ and different values of E_{tag} and ρ. We have chosen $\theta_{tag} > 30\,\mathrm{mrad}$, the other cuts are as above. Given are numbers of events for BFKL and for 2–gluon exchange (in brackets).

numbers look very promising even for the smaller values of ρ. The cross section based upon the BFKL calculation is still a factor of about 15 larger compared to the 2-gluon cross section. Requiring larger E_{tag} values reduces the cross section considerably, but the

event rate remains large enough to allow for a study of the BFKL Pomeron at the 500 GeV e^+e^- Linear Collider.

5 Summary

In summary, we have estimated the total cross section of $\gamma^*\gamma^*$ scattering at the designed 500 GeV e^+e^- Linear Collider. At high energies, this subprocess is dominated by the BFKL Pomeron and therefore provides an ideal test of this QCD calculation. A rough estimate of the diffusion in $\log k_T^2$ shows that, at the high energy tail of this subprocess, corrections to the BFKL become non-negligible, and hence deviations from the BFKL power law may become visible.

For a realistic estimate of the number of observable events we find a strong dependence on detector restrictions. In order to have a sufficiently large number of events, especially when applying the additional requirement that the photon virtualities are approximately equal, it is necessary to tag both leptons close to the beam direction. An angle of 30 mrad might already lead to good results, even better would be 20 mrad. For this measurement it is however not sufficient to have only the main detector, which can accept electrons with an angle larger than 80 mrad only, since it leads to too small event rates.

Although the measurement is still feasible for 100 GeV, the energies of the tagged leptons should better go down to about 20 GeV. In this region the 500 GeV e^+e^- Linear Collider provides an excellent possibility for testing the BFKL Pomeron.

References

[1] E. A. Kuraev, L. N. Lipatov, V. S. Fadin, *Sov. Phys. JETP* **45** (1977) 199;
Ya. Ya. Balitskii, L. N. Lipatov, *Sov. J. Nucl. Phys.* **28** (1978) 822.

[2] A. H. Mueller, *Nucl. Phys. B* (Proc. Suppl.) **18C** (1991) 125;
J. Bartels, A. De Roeck, M. Loewe, *Z. Phys.* **C54** (1992) 635;
J. Bartels, M. Besancon, A. De Roeck, J. Kurzhoefer, in *Proceedings of the HERA Workshop 1992* (eds. W. Buchmüller and G. Ingelman), p.203;
J. Kwiecinski, A. D. Martin, P. J. Sutton, *Phys. Lett.* **B 287** (1992) 254; *Phys. Rev.* **D 46** (1992) 921;
W.-K. Tang, *Phys. Lett.* **B 278** (1991) 363.

[3] J. Bartels and H. Lotter, *Phys. Lett.* **B 309** (1993) 400.

[4] J. Bartels, H. Lotter, M. Vogt, *Phys. Lett.* **B 373** (1996) 215.

[5] J. Bartels, V. DelDuca, A. De Roeck, D. Graudenz, M. Wüsthoff, *Phys. Lett.* **B 384** (1996) 300.

[6] S. Wölfle, talk presented at *Deep Inelastic Scattering and Related Phenomena (DIS 97)*, April 1997, Chicago

[7] A. De Roeck, in *Deep Inelastic Scattering and Related Phenomena (DIS 96, Rome)*, World Scientific, p. 486

[8] J. Bartels, A. De Roeck, H. Lotter, *Phys. Lett.* **B 389** (1996) 742.

[9] S. J. Brodsky, F. Hautmann, D. E. Soper, *Phys. Rev. Lett.* 78 (1997) 803, S. J. Brodsky, F. Hautmann, D. E. Soper, SLAC-PUB-7480, hep-ph/9706427, to be published in *Phys. Rev.* **D**

[10] A. Bialas, W. Czyz, W. Florkowski, *Phys. Rev.* **D 55** (1997) 6830.

[11] OPAL Collaboration, K. Ackerstaff et al., CERN-PPE/97-103.

[12] Report on the Conceptual Design of 500 GeV e^+e^- Linear Collider with Integrated X–Ray Laser Facility, Eds. R. Brinkmann, G. Materlik, J. Rossbach and A. Wagner, DESY 1997-048 and ECFA 1997-182.

[13] D. Schulte, PhD. Thesis, DESY/Hamburg University 1997, TESLA note 97-08.